AERODYNAMIC AND AEROACOUSTIC CHARACTERISTICS OF FLATBACK AIRFOILS FOR USE ON LARGE WIND TURBINES

Tae Hyung Kim[a*], Min U Jeon[a], Hyung Ki Shin[b], and Soo Gab Lee[a]

[a] *Department of Mechanical and Aerospace Engineering, Seoul National University, Seoul,151-742, Korea*

[b] *Distributed Power Generation and Energy Storage Department, Korea Institute of Energy Research, Daejeon, 305-343, Korea*

[*] *Correnspondingauthor:Tel.:+82-2-880-7299; fax:+82-2-876-4360*

E-mail address : zestriver@snu.ac.kr

ABSTRACT

The present paper presents a possible path for developing a large eddy simulation (LES) applicable to high Reynolds-number complex turbulent flows, performance of the coupling of LES with statistical turbulence models, i.e. Reynolds-Averaged Navier-Stokes (RANS) modeling around the flow over a blunt trailing edge configuration was investigated. To discuss the model performance in detail, LES, RANS and embedded LES models were applied to a three-dimensional turbulent flow around a flatback airfoil with massive separation. The hybrid LES/RANS model gave considerable improvement of the prediction accuracy even with moderate grid resolution. The turbulent fluctuations in the boundary layers at the inflow region of the LES domain are generated by synthetic vortex method. The comparison with RANS and LES solution for the full domain and with experimental data shows likewise results for the pressure distributions surrounding flatback airfoils. To predict accurately the noise radiation from the blunt trailing edge and to save computational costs, the near field region is computed by embedded LES and the other surrounding region is computed by RANS simultaneously. The present hybrid LES/RANS method is found to be adequate for predicting noise radiation over a range of frequencies.

KEYWORDS

Large eddy simulation, Hybrid LES/RANS model, Synthetic vortex method, Three-dimensional flatback airfoil, Separation, Near-wall turbulence

NOMENCLATURE

LES	large eddy simulation
RANS	Reynolds-averaged Navier-Stokes
2D, 3D	tow-, three-dimensional
C_p	pressure coefficient
M	Mach number
Re	Reynolds number
U	mean velocity

j	number of grid-line
k	turbulent kinetic energy
l	turbulent length-scale
p	pressure
r	distance
t	time
u, v, w	velocity components
x, y, z	Cartesian coordinates
ε	turbulent dissipation rate
ρ	density
σ	size of vortex

1. INTRODUCTION

The inboard region of large wind turbine blades requires thick airfoils to meet structural requirements. The use of flatback airfoils permits the use of increased thickness airfoils without the chord increases that would occur if conventional thick airfoils were used. Avoiding this additional chord length makes the resulting structural design more compact and easier to construct, resulting in a blade that is transported with facility [1]. Despite many kinds of benefits such as structural improvements, high sectional lift coefficients and reduction of sensitivity to leading edge surface soiling the flatback airfoils are considered to induce increased blade drag and trailing edge vortex shedding noise. For high Reynolds number, the wake of flataback airfoils is accompanied by three dimensional instabilities which emerge as pairs of counter-rotating streamwise vortices connecting the von Karman vortices. These three dimensional instabilities are dependent on Reynolds number, free stream turbulence and the turbulent layer boundaries at the two ends of the three dimensional blunt trailing edge profiled body [2].

Large eddy simulation (LES) is well known as a useful tool to predict practical turbulent problems. Although LES needs far fewer grid nodes compared to direct numerical simulation (DNS), there still remains serious difficulties in its application to high Reynolds-number flows. In the LES concept only the dissipative scales of turbulence, which are assumed to have a more isotropic character than large scales in a shear-driven flow, are modeled while the eddies carrying the bulk of energy of the flow are resolved. However, in the near wall region the number of grid points increases drastically because the temporal and spatial scales of the energy containing eddies become very small. Therefore, LES cannot be applied to large scale flow problems.

To overcome these difficulties, the hybrid RANS/LES model which is originally based on the concept of a hybrid model connecting LES with Reynolds-Averaged Navier-Stokes (RANS) modeling in the near wall region is emerged. A number of researchers have performed this concept

(Davidson and Peng, 2003 [3]; Hanjalic et al., 2004 [4]; Temmerman et al., 2005 [5]; Ken-ichi Abe et al., 2010 [6]). Every approach has provided encouraging results and useful knowledge for further development of this field. On the other hand, very few studies, which include a detailed description of the near-wall turbulence and acoustic prediction when the hybrid RANS/LES models are applied to flow and noise predictions.

Segregated modeling has opposite meaning to unified modeling such as RANS, LES, and DNS. In the segregated modeling, LES is employed in one part of the computational domain, while RANS is used in the remainder [7]. The resolved quantities are no more continuous at the RANS/ LES interfaces. Instead, almost independent LES and RANS computations are performed in their respective subdomains. Then the computed results are matched through appropriate boundary conditions. The embedded LES method is a kind of segregated modeling and is composed of full two-way coupling between RANS and LES zones. The LES-inflow boundary of an LES embedded in a RANS solution is assumed to be steady. The steady RANS solution does not provide any turbulent fluctuations. Performing LES on the downstream side of the RANS interface requires proper LES-boundary conditions. In this study, a synthetic vortex method [8] is used to generate the turbulent fluctuations at the explicit RANS/LES interface and this method is validated as a relative inexpensive and accurate approach to generate fluctuations representing a turbulent flow field at the inlet of a LES domain.

The present paper is a contribution to the ongoing research for a better turbulence model applicable to complex turbulent flows and aero-acoustic prediction of flatback airfoils with moderate computational cost. Aerodynamic measurements were made in this experiments for comparison with computational results. The noise prediction of flatback airfoils for large wind turbines are obtained using a hybrid LES/RANS method and Ffowcs Williams-Hawkings equation.

2. METHODOLOGY

2.1 Segregated modeling

Segregated modeling for hybrid RANS/LES methods is based on decomposing the entire domain before starting the simulation into clearly identifiable regions for RANS and LES. The connection between the distinct zones during the simulation is established via explicit coupling of the solution, i.e. velocities and pressure, at the interfaces. Though the coupling has to be two-way with exchange in both direction for a true RANS/LES hybrid method, the problem is reduced to a standard LES setup, where the RANS solution can be computed a priori and only serves to provide better boundary conditions.

At inflow-type interfaces, mass, momentum, energy, flow structures, etc. are convected from a RANS region into the subdomain treated by LES. The mean values are provided by the RANS calculation and coupled to the explicitly averaged LES data. If very strong instabilities exist inside

the LES domain and the upstream unsteadiness has only little impact to the downstream flow, this might already suffice. The LES requires the provision of fluctuations at the interface in order to avoid an artificial transition zone in the LES subdomain. To this end, methods applicable for pure LES can be used.

Two classes of unsteady inflow data can be distinguished: real unsteady flow structures and artificial fluctuations, where the latter can be seen as a model of the first. Real flow structures can be provided in several ways: specifically designed precursor simulations or databases for similar flows with additional adjustment. Synthetic turbulent fluctuations can be obtained by various strategies: proper orthogonal decomposition (POD) modes, Fourier modes, digital filters, random vortices, stochastic forcing, etc. Imposing fluctuations as close as possible to those present in the real flow is crucial. Otherwise they will be damped rapidly, hence failing the purpose of the method.

For any RANS zone downstream of an LES zone the primary task of a hybrid RANS/LES coupling at an outflow-type interface is to propagate mean flow information upstream. At the same time, for flows with stationary statistics, the LES should provide only mean flow data to the RANS domain. Since the LES delivers unsteady data, the interface has to allow for the fluctuations to leave the LES domain without reflections.

2.2 Vortex method

The most critical interface is the interface where the flow leaves the RANS domain and enters the LES region (RANS/LES interface). At this interface, it is necessary to convert modeled turbulence kinetic energy into resolved energy for this transfer by an appropriate method. The vortex method [8] is selected for generating resolved turbulence at inlets. To generate a time-dependent inlet condition, a random 2D vortex method is considered. With this approach, a perturbation is added on a specified mean velocity profile via a fluctuating vorticity field. The vortex method is based on the Lagrangian form of the 2D evolution equation. These particles, or "vortex points" are converted randomly and carry information about the vorticity field. If N is the number of vortex points and A is the area of the inlet section, the amount of vorticity carried by a given particle i is represented by the circulation Γ_i and an assumed spatial distribution η :

$$\Gamma_i(x,y) = 4\sqrt{\frac{\pi A k(x,y)}{3N[2\ln(3) - 3\ln(2)]}} \tag{1}$$

$$\eta(\vec{x}) = \frac{1}{2\pi\sigma^2}\left(2e^{-|x|^2/2\sigma^2} - 1\right)2e^{-|x|^2/2\sigma^2} \tag{2}$$

where k is the turbulence kinetic energy. The parameter σ provides control over the size of a vortex particles. The resulting discretization for the velocity field is given by

$$\vec{u}(\vec{x}) = \frac{1}{2\pi}\sum_{i=1}^{N}\Gamma_i \frac{((\vec{x}_i-\vec{x})\times\vec{z})\left(1-e^{|\vec{x}-\vec{x}'|^2/2\sigma^2}\right)}{|\vec{x}-\vec{x}_i'|^2} \quad (3)$$

where $\vec{z}$ is the unit vector in the streamwise direction. Originally, the size of the vortex was fixed by an ad hoc value of σ. To make the vortex method generally applicable, a local vortex size is specified through a turbulent mixing length hypothesis. σ is calculated from a known profile of mean turbulence kinetic energy and mean dissipation rate at the inlet according to the following:

$$\sigma = \frac{ck^{3/2}}{2\varepsilon} \quad (4)$$

where c=0.16. To ensure that the vortex will always belong to resolve scales, the minimum value of σ in (3) is bounded by the local grid size. The sign of the circulation of each vortex is changed randomly each characteristic time scale τ. In the general implementation of the vortex method, this time scale represents the time necessary for a 2D vortex convected by the bulk velocity in the boundary normal direction to travel along n times its mean characteristic 2D size (σ_m), where n is fixed equal to 100 from numerical testing. The vortex method considers only velocity fluctuations in the plane normal to the streamwise direction.

However, a simplified linear kinematic model for the streamwise velocity fluctuations is used. It is derived from a linear model that mimics the influence of the two-dimensional vortex in the streamwise mean velocity filed. If the mean streamwise velocity U is considered as a passive scalar, the fluctuation u' resulting from the transport of U by the planar fluctuating velocity field v' is modeled by

$$u' = -\vec{v}' \cdot \vec{g} \quad (5)$$

where $\vec{g}$ is the unit vector aligned with the mean velocity gradient $\overrightarrow{\nabla U}$. When this mean velocity gradient is equal to zero, a random perturbation can be considered instead. Since the fluctuations are equally distributed among the velocity components, only the prescribed kinetic energy profile can be fulfilled at the inlet of the domain. Farther downstream, the correct fluctuation distribution is recovered. However, if the distribution of the normal fluctuations is known or can be prescribed at the inlet, a rescaling fluctuations <*uu*>, <*vv*>, and <*ww*> as given at the inlet.

With the rescaling procedure, the velocity fluctuations are expressed according to:

$$u_i'^{*} = u_i' \frac{\sqrt{\langle u_i u_i \rangle}}{\sqrt{2/3k}} \quad (6)$$

This also results in an improved representation of the turbulent flow field downstream of the inlet. All calculations have been obtained using the compressible formulation of general-purpose

control-volume code, FLUENT. This code employs a cell-centered finite-volume method based on a multi-dimensional linear reconstruction scheme, which permits use of computational elements with arbitrary topology. In the present study, only hexhedral cells were considered. For the computation presented in this paper, the segregated solver was used. With this solver, the governing equations are solved sequentially. The temporal discretization employs a fully-implicit, three-level second-order scheme.

2.3 The Ffowcs Williams-Hawkings equation

In 1969 Ffowcs Williams and Hawkings published their now classic paper "Sound Generation by Turbulence and Surfaces in Arbitrary Motion" which generalized Lighthill's acoustic analogy approach to include the effects of very general types of surfaces and motions. Using the mathematical theory of distributions, they were able to rearrange the Navier-Stokes equations into the form of an inhomogeneous wave equation with a quadrupole source distribution in the volume surrounding the body and monopole and dipole sources on the body surface. The Ffowcs Williams-Hawkings (FW-H) equation can be written in differential form as

$$\overline{\square}^2 p'(x,t) = \frac{\partial}{\partial t}\{[\rho_0 v_n + \rho(u_n - v_n)]\delta(f)\} - \frac{\partial}{\partial x_i}\{[\Delta P_{ij}\hat{n}_j + \rho u_i(u_n - v_n)]\delta(f)\} + \frac{\partial^2}{\partial x_i \partial x_j}[T_{ij}H(f)] \quad (7)$$

where $T_{ij} = \rho u_i u_j + P_{ij} - c^2\rho'$ is the Lighthill stress tensor ($\rho'=\rho-\rho_0$) and on the left side we use the notation $\overline{\square}^2 = [(1/c^2)(\partial^2/\partial t^2)] - \overline{\nabla}^2$ is the local velocity of the body in the direction normal to the surface implicitly defined by f=0, l_i are the components of the local force on the surface, δ(f) and H(f) are the Dirac delta and Heaviside functions, respectively. P_{ij} is the compressive stress tensor. For a Stokesian fluid, this is given by

$$P_{ij} = p\delta_{ij} - \mu\left[\frac{\partial u_i}{\partial x_j} + \frac{\partial u_j}{\partial x_i} - \frac{2}{3}\frac{\partial u_k}{\partial x_k}\delta_{ij}\right] \quad (8)$$

The first source term is monopole (thickness) source and the second source term is dipole (loading) source based on their mathematical structure. Both of these sources are surface sources. The third source term is a quadrupole source term that acts throughout the volume that is exterior to the data surface. The monopole or thickness source term models the noise generated by the displacement of fluid as the body passes. The dipole or loading source term models the noise that results from the unsteady motion of the force distribution on the body surface. The thickness and loading source terms have been used for several years in rotor noise prediction because they account for most of the acoustic signal when the flow field is not transonic or supersonic. Furthermore, they do not require knowledge of the flow field off the blade (although the accurate

determination of the blade-surface pressure is still challenging).

The quadrupole source term models the non-linearities due to both the local sound speed variation and the finite fluid velocity near the blade. The quadrupole source has often been neglected in rotor noise prediction because of the computational demands of determining the flow field with sufficient accuracy to be used for noise prediction and the computational challenge of volume integration in the acoustic prediction. In this paper, the prediction of volume noise source is not considered.

The speed and accuracy of the noise calculation is improved by elimination of the time derivative of the first integral in Formulation 1. Using the definition of the retarded time function g and the fact that r is a function of τ gives

$$\left.\frac{\partial}{\partial t}\right|_X = \left(\frac{1}{1-M_r}\left.\frac{\partial}{\partial t}\right|_X\right)_{ret} \tag{9}$$

where the $|_x$ implies that the observer position x is fixed during the differentiation. The final result is

$$p'(\mathbf{x},t) = p'_T(\boldsymbol{x},t) + p'_L(\boldsymbol{x},t) \tag{10}$$

where

$$4\pi p'_T(\boldsymbol{x},t) = \int_{f=0}\left[\frac{\rho_0(\dot{v}_n + v_{\dot{n}})}{r|1-M_r|^2}\right]_{ret} dS + \int_{f=0}\left[\frac{\rho_0 v_n\left(r\dot{M}_r + cM_r - cM^2\right)}{r^2|1-M_r|^3}\right]_{ret} dS \tag{11}$$

$$\begin{aligned} 4\pi p'_L(\boldsymbol{x},t) = {} & \frac{1}{c}\int_{f=0}\left[\frac{\dot{l}_r}{r|1-M_r|^2}\right]_{ret} dS + \int_{f=0}\left[\frac{l_r - l_M}{r|1-M_r|^2}\right]_{ret} dS \\ & + \frac{1}{c}\int_{f=0}\left[\frac{l_r\left(r\dot{M}_r + cM_r - cM^2\right)}{r^2|1-M_r|^3}\right]_{ret} dS \end{aligned} \tag{12}$$

which is known as Formulation 1A. In these equations a dot over a variable implies the source time derivative of that variable and the subscript *n*, *r* and *M* refer to the dot product with the unit normal vector, the unit radiation vector, or the surface velocity vector normalized by the speed of sound, respectively. In this formulation, integrands with *1/r* dependence are far-field terms and those with $1/r^2$ dependence are near-field terms.

3. TEST CASE AND COMPUTATIONAL CONDITIONS

The test flatback airfoils are categorized by two groups. The first airfoil group is composed of DU97-W-300 and DU97-flatback airfoils. This group is tested for aeroacoustic characteristics. The second airfoil group contains KWA029-400. This airfoil is tested for the similarities and differences of aerodynamic performances between numerical approaches and experiments. The numerical approaches are X-foil panel method, RANS, LES, and hybrid LES/RANS methods.

The blunt trailing edge profiled body geometry for the numerical model for the first airfoil

group, which has a thickness to chord ratio of t/c = 12.5, is the similar to the one studied by Barone et al. (2010) [9]. The baseline airfoil is TU-Delft DU97-W-300 which has a sharp trailing edge thickness of t/c = 1.7, while the modified airfoil is TU-Delft DU97-flatback which has a flatback version trailing edge thickness of t/c = 10, as shown in Fig. 1. The chord length of the profiled body in the numerical solution is $c = 0.91m$. The numerical simulations are carried at Re(c) = 3,000,000 for angle of attack 4°.

The solution domain is defined as a tetrahedral volume surrounding the profiled body. The domain extends 10c behind, 10c in front, and 10c from the upper and lower surfaces of the body. The region surrounding the solid walls of the body is discretized using a boundary layer-type structured grid of hexahedral cells, which are refined towards the wing surfaces. The remaining part of the solution domain, which encompasses the inner region, is discretized using an unstructured grid of tetrahedral cells. The grid size has been previously increased in steps of +9%. The close up views of the final hybrid grids, which has 2.9×10^5 cells for RANS domain and 3.9×10^6 cells for LES domain, are shown in Fig. 2 for DU97-W-flatback. The numerical solutions are validated through the test which were performed in the Virginia Tech Stability Wind Tunnel, a continuous, single return, subsonic wind tunnel with a 1.83-m (6-ft) square, 7.3-m (24-ft) long removable rectangular test section. Details of the numerical solution procedure are provided in the paper by Berg. et al [10].

The second group flatback airfoil body geometry for the numerical model and experimental model is KWA029-400 which is the test model developed by KIER(Korea Institute of Energy Research) (Fig. 3). As it is not shown here, the experimental facility has a long constant rectangular cross-section duct of heigh $1.25m$ and width $1.249m$, resulting in a fully-developed turbulent flow at the end of the inlet rectangular duct. The Reynolds number is 10^6 based on the airfoil chord length and the bulk-mean inflow velocity. The chord length of the flatback airfoil body is $0.35m$. The test angle of attack is 0°. The segregated implicit scheme based on the SIMPLE algorithm, which is available in the commercial CFD program FLUENT, has been used for solution of the governing equations in three dimensions. Temporal discretization is performed using a time step size of 1.0×10^{-5}sec.

4. RESULTS

4.1 Aerodynamic results

Some illustrative results of the hybrid LES/RANS computations are shown below in Fig. 4. In this figure, the contours of static pressures and velocities are plotted around the airfoil on the $z = 0$ plane. The wake patterns behind the airfoil clearly indicate the wake location and the presence of Karman vortex structures near trailing edge. The vorticity contours also provide a clear picture of the turbulence which convects past the blunt trailing edge in Fig. 5. In the following sections, both

aerodynamic and aeroacoustic results from the RANS, LES, and hybrid LES/RANS simulations will be evaluated against experimental data.

Quantitative comparisons of the airfoil's aerodynamic performance, in terms of pressure distributions, are shown in Fig. 6. The distribution of the pressure coefficient, defined as $C_p = 2(p-p_\infty)/\rho U^2_\infty$, is plotted alongside predictions from the XFOIL panel method [11] and experimental data from KIER. Good agreement among the RANS, hybrid LES/RANS, LES, XFOIL, and the KIER experimental data is seen on both the suction side and the pressure side of the airfoil.

4.2 Aeroacoustic results

The far-field acoustics from the semi-empirical calculations for DU97-W-300 and DU97-flatback airfoils were compared against corresponding experimental data. The empirical expression for the blunt trailing edge vortex shedding noise was determined using the predicted data of Brooks and Hodgson [12], and is valid for turbulent, NACA0012 airfoil boundary layer flows.

$$SPL_{BLUNT} = 10\log\left(\frac{hM^{5.5}\Delta L\overline{D}_h}{r^2}\right) + G_4\left(\frac{h}{\delta^*_{avg}}, \Psi\right) + G_5\left(\frac{h}{\delta^*_{avg}}, \Psi, \frac{St'''}{S'''_{peak}}\right) \quad (13)$$

where the distance from the trailing edge to the observer is r, the boundary layer thickness δ^* is taken to the average of the suction and pressure side thickness. The non-dimensional frequency was defined as $St = f\delta^*/U_\infty$ given the frequency f in Hertz.

For the far field acoustics, the sound pressure level were recorded in the prediction codes at the same observer locations as the Virginia Tech experiments. The experiments at Virginia Tech tested DU97-W-300 airfoil and DU97-flatback airfoil with a chord length of 0.91m, angle of attack of 4.0 degrees, velocity of 56.5 m/s (Re=.30 million), and with a far-field measurement location that was situated on the midspan-plane, 3.12 m from the trailing edge and 112.0 degrees from the streamwise axis.

Some acoustic results of the hybrid LES/RANS computations are shown in Fig. 7. In this figure, the acoustic pressure signals and drag and lift time history are plotted at the same observer location with the experiments. Noise prediction is calculated from t = 0.07s after initial transients have been washed out in Fig. 7 (b).

The results of these aeroacoustic comparisons are shown in Fig. 8, which shows the predicted far-field noise by the hybrid LES/RANS computation at the same locations as in the experiments and with the same frequency averaging (Narrowband). The numerical results by semi-empirical formula is shown with 1/3-octave band frequency due to the limits of prediction codes. The difference at low frequencies between semi-empirical formula and experimental measurements was caused by the lack of turbulence inflow noise calculation. For the hybrid LES/RANS computation, good agreement is seen for the peak frequencies(150~200 Hz) of blunt trailing edge noise, and

similar SPL rates of change at lower frequencies. Overall, the difference in SPL between numerical predictions and experimental measurements was within 10 dB for medium to higher frequencies.

5. DISCUSSION AND CONCLUSIONS

LES, RANS, and hybrid LES/RANS have been carried out for turbulent boundary-layer flows past blunt trailing edges of several flatback airfoils at a chord Reynolds number of 1.0×10^6 and 3.0×10^6. The computed pressure distributions by LES and hybrid LES/RANS simulations compare more reasonably well with the experimental measurements of KIER than the results by XFOIL and RANS computation. The discrepancies observed at some trailing edge stations may have been caused by inadequate inflow velocity conditions, small computational spanwise domain size, as well as high vortex sheddings near the blunt trailing edge.

The objectives of the trailing-edge flow by hybrid LES/RANS are to predict the space-time characteristics of surface pressure fluctuations and to provide the acoustic source functions for the far-field noise calculation. The frequency spectra of surface pressure fluctuations obtained from the hybrid LES/RANS agree well with experimental measurements at the same observer location. The cause for the over-prediction at high frequencies needs to be further investigated.

The far-field acoustics is computed from an integral form solution to the Lighthill equation developed by Ffowcs-Williams and Hawkings. The acoustic evaluation is performed in the Fourier frequency domain using source-field data obtained from the hybrid LES/RANS. To predict accurately the noise radiation from the blunt trailing edge and to save computational costs, the near field region is computed by embedded LES and the other surrounding region is computed by RANS simultaneously. The present hybrid LES/RANS method is found to be adequate for predicting noise radiation over a range of frequencies. At the peak frequency and peak level of blunt trailing edge vortex shedding noise, however, the estimation based on surface pressure fluctuations is not matched with the experimental measurements exactly. This issue will be addressed in future simulations using an expanded computational domain and an improved inflow velocity condition.

6. ACKNOWLEDGEMENT

This work was supported by the Human Resources Development program (No. 20104010100490) of the Korea Institute of Energy Technology Evaluation and Planning (KETEP) grant funded by the Korea government Ministry of Knowledge Economy.

7. REFERENCES

[1] Ashwill, T., Laird, D., Concepts to facilitate very large blades, *Proceedings, ASME/AIAA Wind Energy Symposium* 2007, Reno, NV.

[2] Oertel, Jr. H., Wakes behind blunt bodies, *Annual Review in Fluid Mechanics* 1990; 22; 539-564.

[3] Davidson, L., Peng, S. H., Hybrid LES-RANS modeling: a one-equation SGS model combined with a k-ω model for predicting recirculating flows, *Int. J. Number. Meth. Fluids* 2003; 43; 1003-1018.

[4] Hanjalic, K. et al., Merging LES and RANS strategies: zonal or seamless coupling, *Direct and Large Eddy Simulation Kluwer Academic Publ.* 2004; 5; 451-464.

[5] Temmerman, L. et al., A hybrid two-layer URANS-LES approach for large eddy simulation at high Reynolds numbers, *Int. J. Heat Fluid Flow* 2005; 26; 173-190.

[6] Ken-ichi Abe et al., An investigation of LES and hybrid LES/RANS models for predicting 3-D diffuser flow, *Int. J. Heat Fluid Flow* 2010; 31; 833-844.

[7] Fröhlich J., von Terzi D., Hybrid LES/RANS methods for the simulation of turbulent flows, *Progress in Aerospace Sciences* 2008; 44; 349-377.

[8] Mathey F. et al., Specification of LES inlet boundary condition using vortex method, *4th International Symposium on Turbulence, Heat and Mass Transfer* 2003, Antalya, Turkey, Begell House, Inc.

[9] Barone M., Paquette J., Aeroacoustics and aerodynamic performance of a rotor with flatback airfoils, *European Wind Energy Conference* 2010, Warsaw, Poland

[10] Berg, D. E., Zayas, J. R., Aerodynamic and aeroacoustic properties of flatback airfoils, *46th AIAA Aerospace Sciences Meeting and Exhibit* 7-10 January 2008, Reno, Nevada

[11] Drela, M., *XFOIL: An Analysis and Design System for Low Reynolds Number Airfoils, Low Reynolds Number Aerodynamics*, University of Notre Dame Press, 1-12, 1989

[12] Brooks, T. F., Hodgson, T. H., Trailing edge noise prediction from measured surface pressure, *Journal of Sound and Vibration* 1981; 78(1); 69-117

Figures

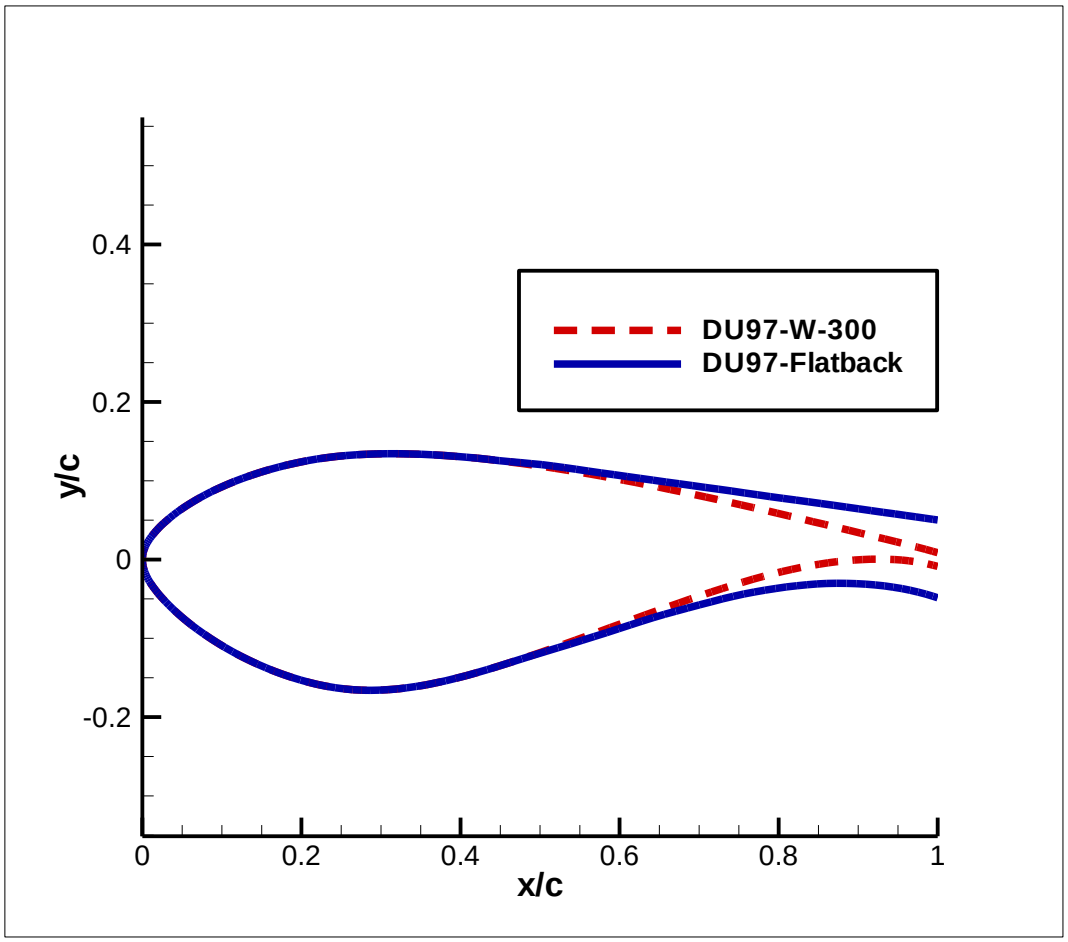

Fig. 1 A cross section of the DU97-W-300 and DU97-flatback airfoil geometry

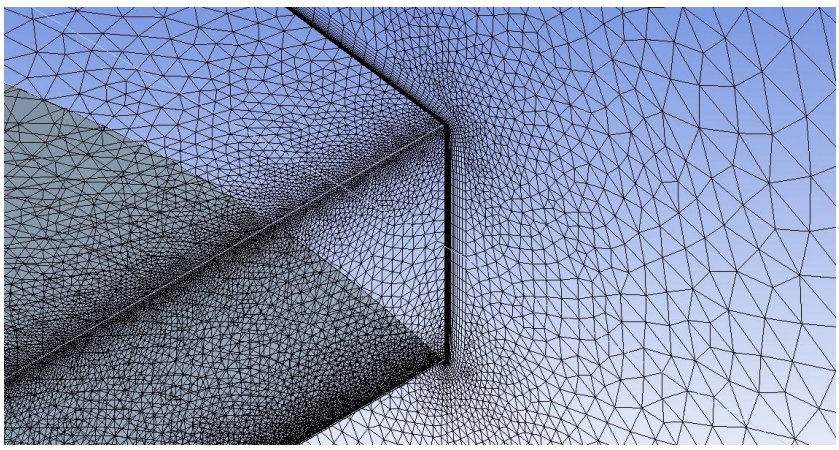

Fig. 2 Close-up view of the mesh near the DU97-flatback airfoil trailing edge

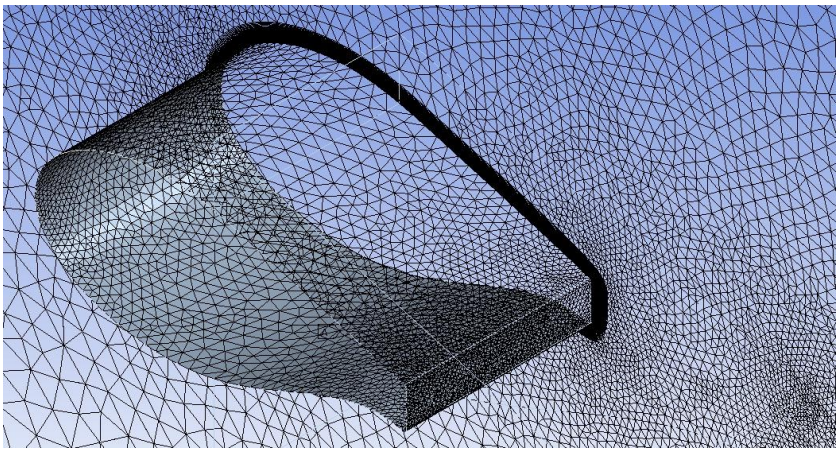

Fig. 3 The unstructured mesh for the computational domain and refined region surrounding the KWA029-400 airfoil

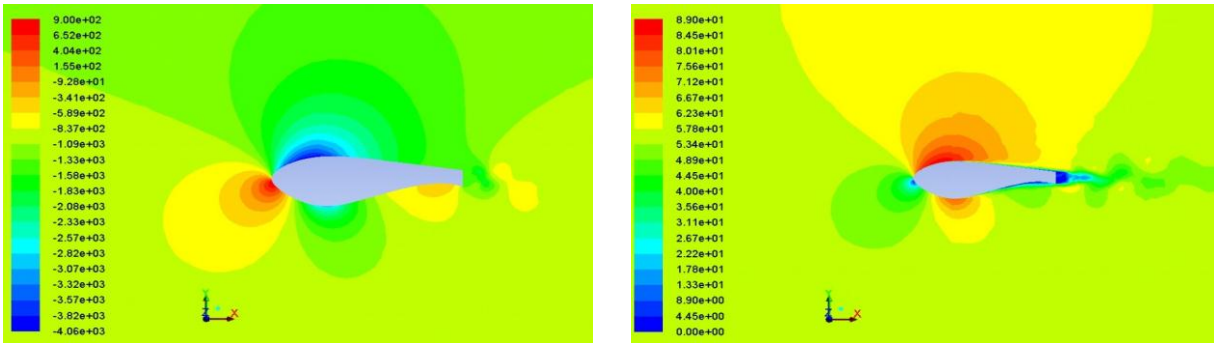

(a) (b)

Fig. 4 (a) The pressure distribution and (b) the velocity field surrounding the DU97-flatback airfoil

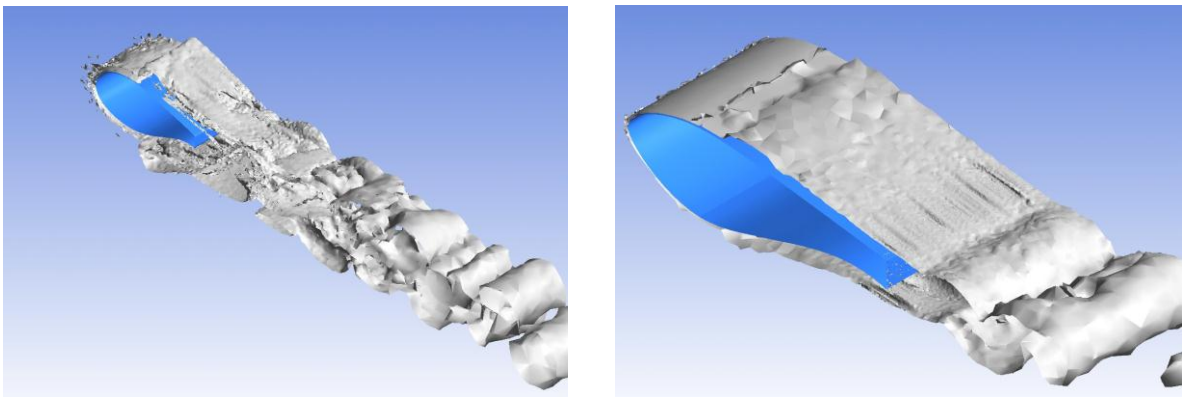

(a) (b)

Fig. 5 Instantaneous snapshot of the fluid vorticity in the near-field domain computed by (a) hybrid LES/RANS and (b) full LES

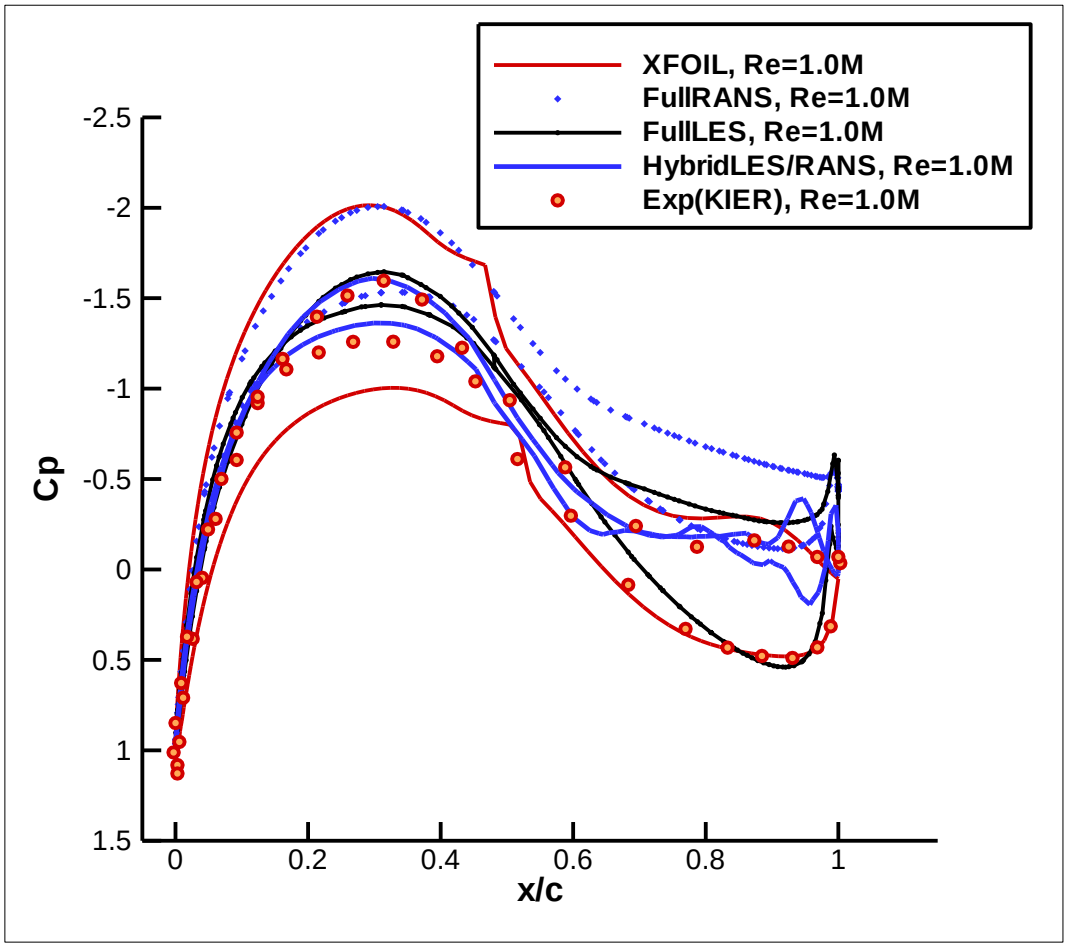

Fig. 6 A comparison of the pressure coefficient C_p between the XFOIL predictions, RANS simulation, LES simulation, hybrid LES/RANS simulation, and experimental data

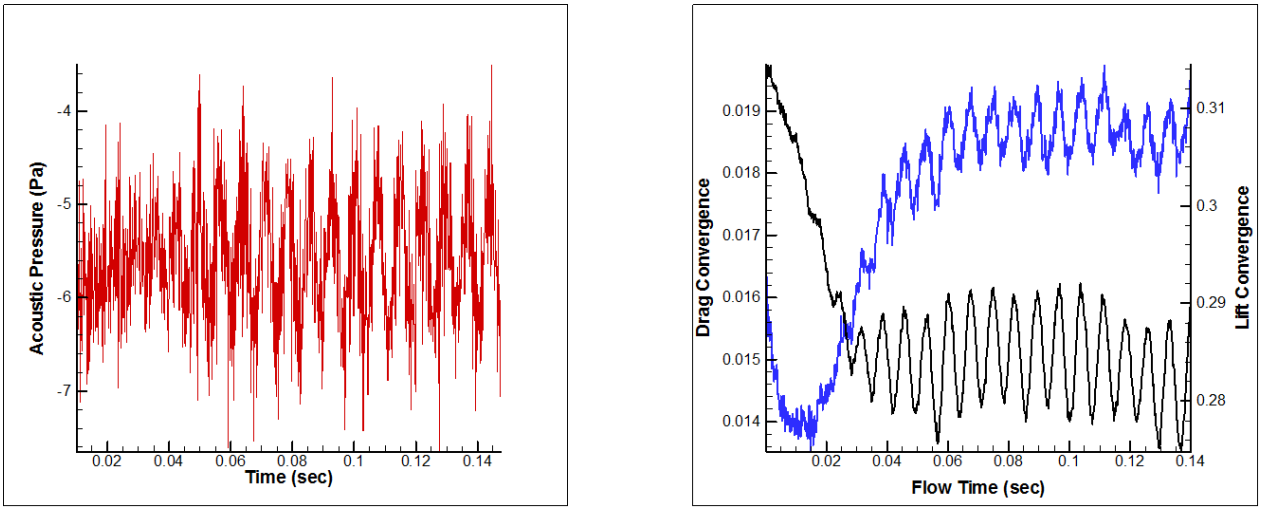

(a) (b)

Fig. 7 Acoustic results by the hybrid LES/RANS simulation: (a) acoustic pressure signal and (b) drag and lift convergence time history

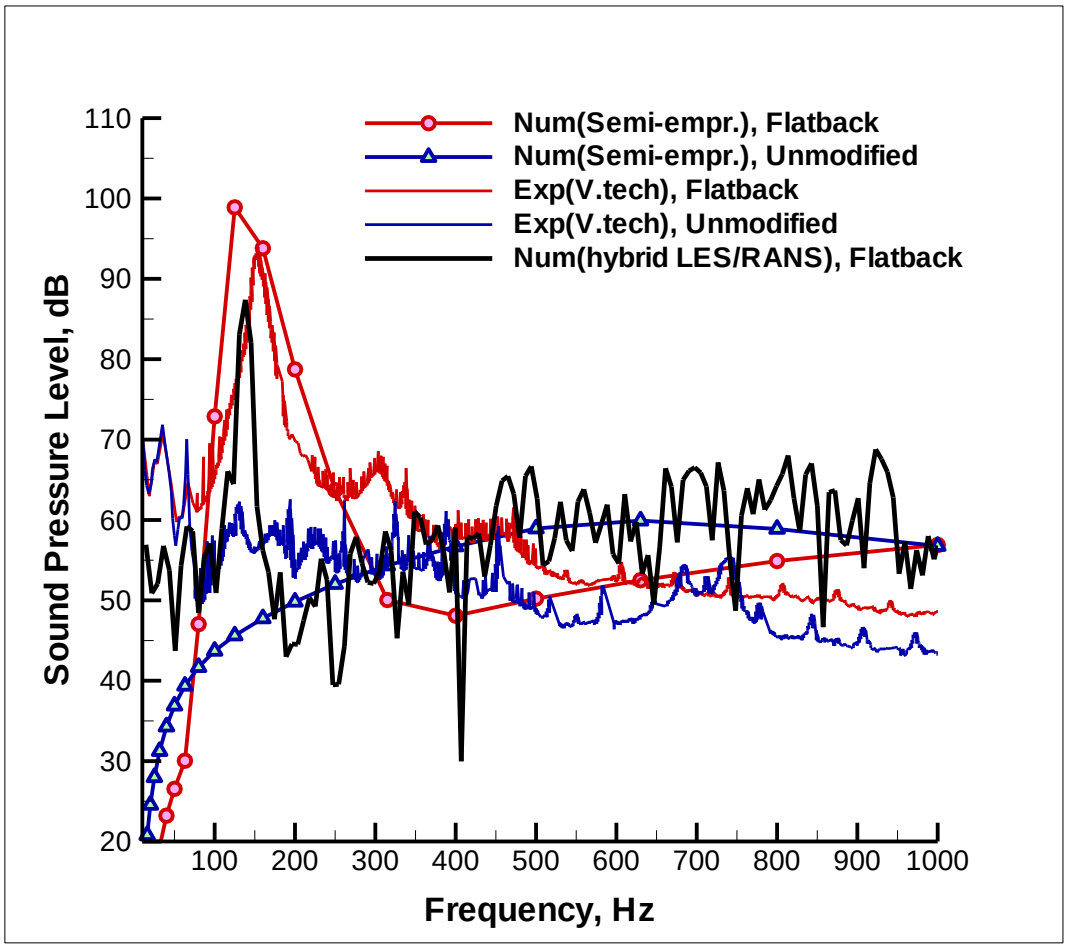

Fig. 8 A comparison between the far-field measurements obtained from the Virginia Tech. experiments, and the corresponding SPL calculated from the hybrid LES/RANS data and the semi-empirical formula at the same observer position as the experiment for DU97-W-300 and DU-flatback airfoils